

Quantum Error Correction near the Coding Theoretical Bound

Daiki Komoto¹ and Kenta Kasai¹

¹ Institute of Science Tokyo
2–12–1 Ookayama, Meguro-ku, Tokyo, 152–8550, Japan
{komoto.d.aa, kasai.k.ab}@m.titech.ac.jp.

Submitted on December 31, 2024

Abstract

Recent advancements in quantum computing have led to the realization of systems comprising tens of reliable logical qubits, constructed from thousands of noisy physical qubits [1]. However, many of the critical applications that quantum computers aim to solve require quantum computations involving millions or more logical qubits [2, 3]. This necessitates highly efficient quantum error correction capable of handling large numbers of logical qubits. Classical error correction theory is well-developed, with low-density parity-check (LDPC) codes [4] achieving performance limits by encoding large classical bits [?]. Despite more than two decades of effort, no efficiently decodable quantum error-correcting code that approaches the hashing bound [6, 7, 8], which is a fundamental lower bound on quantum capacity, had been discovered. Here, we present quantum error-correcting codes constructed from classical LDPC codes that approach the hashing bound while maintaining linear computational complexity in the number of physical qubits. This result establishes a pathway toward realizing large-scale, fault-tolerant quantum computers. By integrating our quantum error correction scheme with devices capable of managing vast numbers of qubits, the prospect of solving critical real-world problems through quantum computation is brought significantly closer.

1 Introduction

Recent progress in quantum computing has enabled the development of systems with tens of reliable logical qubits, built from thousands of noisy physical qubits [1]. Nonetheless, many essential applications targeted by quantum computers demand quantum computations that involve millions or even more logical qubits [2, 3]. This creates a pressing need for highly efficient quantum error correction methods that can accommodate a vast number of logical qubits.

A classical error-correcting code defined by a sparse parity-check matrix is called a low-density parity-check (LDPC) code. It is known that LDPC codes achieve error correction performance that approaches the channel capacity with computational complexity proportional to the code length in classical error correction [4].

Protograph codes [9] are LDPC codes whose parity-check matrices are constructed using a protograph matrix composed of permutation matrices as submatrices. A subclass of these codes includes quasi-cyclic (QC) LDPC codes [10], which are constructed using circulant permutation matrices (CPMs), and APM-LDPC (affine permutation matrices) codes [11], which are constructed using APMs. Similar to unstructured LDPC codes, protograph codes are also known for their excellent error correction performance.

Short cycles are particularly known to cause a high error floor. The error floor of LDPC codes refers to a phenomenon where the error rate does not decrease as rapidly as expected with decreasing noise levels, especially in the high-fidelity regime. In computational error correction, extremely low error rates are required, making it critically important to address the error floor phenomenon. It is known that the girth (the length of the shortest cycle) of QC-LDPC matrices is upper-bounded by 12 [10]. However, APM-LDPC matrices can exceed this upper bound on girth [11, 12].

LDPC codes are typically defined over a binary finite field. Certain types of LDPC codes are known to achieve further improvements in error-correcting performance by applying extensions to non-binary finite fields [13], although this increases the computational complexity required for decoding.

Determining the maximum rate at which information can be reliably transmitted through a quantum channel remains one of the most challenging problems in quantum information theory. Specifically, this concerns the concept of quantum channel capacity, which quantifies the maximum rate of quantum information that can be transmitted while preserving its integrity. Even for simple and widely studied noise models, such as the depolarizing channel, the exact value of this capacity is unknown. The most basic lower bound, known as the hashing bound or the LSD theorem [6, 7, 8], is particularly notable. For Pauli channels, this bound has a straightforward expression and can be achieved using random stabilizer codes. It is recognized as a fundamental benchmark for evaluating quantum error correction performance.

The Calderbank-Shor-Steane (CSS) codes [14, 15] are a class of quantum error-correcting codes constructed from a pair of classical error-correcting codes. CSS codes are derived from two classical codes with parity-check matrix pairs (H_X, H_Z) that satisfy the orthogonality condition $H_X H_Z^T = 0$. Each matrix represents the parity-check matrix of one of the classical codes in the pair.

CSS codes defined by orthogonal sparse parity-check matrix pairs are referred to as LDPC-CSS codes. Since LDPC-CSS codes are decoded using algorithms similar to those for classical LDPC codes, they are particularly promising for practical application in large-scale quantum computers. Algebraic construction methods allow for the straightforward construction of orthogonal pairs of QC-LDPC matrices [16].

Kasai et al. [17] successfully constructed finite field extended orthogonal non-binary QC-LDPC matrix pairs from the orthogonal QC-LDPC matrix pairs proposed by Hagiwara et al. [16]. To the best of our knowledge, such codes exhibit quantum error-correcting performance that is closest to the hashing bound. However, since the

girth of the original QC-LDPC codes is upper-bounded by 12 [10], these codes also exhibited a high error floor.

To date, in previous studies, no quantum error-correcting codes approaching the hashing bound and decodable with computational complexity proportional to the number of physical qubits had been discovered. This study aims to construct LDPC-CSS codes that simultaneously achieve a deep error floor, approach the hashing bound, and are decodable with computational complexity proportional to the number of physical qubits.

The decoding performance of non-binary LDPC codes is known to be highest when the column weight of the parity-check matrix is two. Furthermore, as this study builds on the finite field extension method [17] for QC-LDPC matrices with a column weight of 2, we focus exclusively on the case where the column weight is two. For LDPC matrices with a column weight of 2, small girth can lead to high error floors. To mitigate the error floor, it is desirable to exceed a girth of 12. To achieve this, it is necessary to extend the method in [17] to apply to protograph matrix pairs, a general class that includes APMs and CPMs.

First, we present a method for constructing orthogonal protograph matrix pairs. Next, we provide an upper bound on the girth of these protograph matrix pairs. Furthermore, we show that the conditions for achieving this upper bound serve as sufficient and necessary conditions for applying finite field extension method. By replacing the finite field components of the extended protograph matrix pairs with the corresponding companion matrices, we obtain binary orthogonal extended matrix pairs that construct the proposed CSS codes.

Furthermore, we employ a decoding algorithm [18] that decodes X and Z errors simultaneously. In this study, we consider a depolarizing channel where X , Y , and Z errors occur with equal probability, resulting in correlated X/Z errors. In [17], X and Z errors were decoded separately without adopting this decoding method. The proposed algorithm is naturally derived as a sum-product algorithm that marginalizes the posterior probability distributions of X and Z errors under the observed syndrome. Numerical experiments revealed that the error correction performance approaches the hashing bound of a depolarizing channel, exhibiting a deep error floor.

The remainder of this paper is organized as follows. In Section 2, we describe the proposed methods for code construction and decoding. Section 3 presents the error correction performance results of the proposed codes. Further details of these sections are provided in the appendix.

2 Methods

In this section, we briefly describe the construction method and decoding method of the proposed code. For further details, please refer to the appendix.

2.1 Code construction method

The proposed quantum error correction uses CSS codes defined by orthogonal \mathbb{F}_2 -valued¹ matrix pairs (H_X, H_Z) , which are obtained through the following three steps:

1. Construct orthogonal sparse binary protograph matrix pairs (\hat{H}_X, \hat{H}_Z) with column weight J , row weight L , and sub-matrix size P .
2. Replace the entries of 1 in \hat{H}_X and \hat{H}_Z with non-zero elements of \mathbb{F}_q to construct orthogonal \mathbb{F}_q -valued matrix pairs (H_Γ, H_Δ) , where $q = 2^e$ and $e > 1$.
3. Replace the non-zero \mathbb{F}_q elements of H_Γ and H_Δ with companion matrices, which are \mathbb{F}_2 -valued submatrices of size $e \times e$, to construct orthogonal \mathbb{F}_2 -valued matrix pairs (H_X, H_Z) . Replace 0 with the zero matrix.

Each step is detailed in the appendix. The resulting orthogonal binary matrix pairs (H_X, H_Z) both are of size $ePJ \times ePL$. These matrix pairs (H_X, H_Z) define the proposed code as orthogonal matrix pairs. Although the proposed code is defined by binary matrix pairs, these matrix pairs can also be interpreted as non-binary \mathbb{F}_q -valued matrices. Thus, the proposed code aims to achieve high decoding performance by treating it as a non-binary LDPC code during decoding.

2.2 Decoding method

It is known that any error occurring in a quantum state can be corrected by addressing both bit-flip and phase-flip errors [19]. Binary CSS codes defined by (H_X, H_Z) correct errors by estimating the error vector $(\underline{x}, \underline{z})$ based on the corresponding syndrome vectors $\underline{s} = H_X \underline{x}$ and $\underline{t} = H_Z \underline{z}$.

The sum-product (SP) algorithm is an efficient algorithm for marginalizing multivariate sparsely-factorized functions defined over a large number of variables [20]. Error correction for the proposed codes is performed as follows. Given the observed syndromes $(\underline{s}, \underline{t})$, the posterior probability distribution of the errors $(\underline{x}, \underline{z})$ are marginalized using the SP algorithm on the sparsely factorized representation. The error estimates $(\hat{\underline{x}}, \hat{\underline{z}})$, which maximize the marginal posterior probability distribution, are then determined.

3 Results

First, we randomly constructed $(\underline{f}, \underline{g})$ to satisfy the conditions (a), (b), and (c) defined in the appendix. Next, we generated (\hat{H}_X, \hat{H}_Z) using the parameters $J = 2$, $L \in \{8, 10, 16\}$, and $P \in \{32, 128, 1024, 8192\}$. These were then extended to (H_Γ, H_Δ) through a finite field extension with $e = 8$ and subsequently converted to (H_X, H_Z) using the companion matrix. We used a $\mathbb{F}_{q=2^e}$ with primitive polynomial $1 + x^2 + x^3 + x^4 + x^8$. You can find these matrices in the file submitted alongside this paper.

The CSS codes defined by (H_X, H_Z) are of coding rate $R = 1 - 2J/L$. As a result, the coding rates of the CSS codes constructed above are $R \in \{0.50, 0.60, 0.75\}$.

¹ $\mathbb{F}_2 = \{0, 1\}$

For the CSS codes defined by (H_X, H_Z) , the quantum error-correction performance over a depolarizing channel was evaluated. The number of physical qubit is given by $n = ePL$.

In a depolarizing channel, the probabilities of X, Y, and Z errors are each given by $p_D/3$. In this case, the marginal probability that either X or Z error occurs is $f_m = 2p_D/3$. The decoding result is defined as successful if the decoding algorithm correctly estimates both error vectors: $\underline{x} = \hat{\underline{x}}, \underline{z} = \hat{\underline{z}}$. If the estimation fails for even a single bit of \underline{x} or \underline{z} , the decoding is considered failed. The frame error rate (FER) is defined as the ratio of the number of experiments where at least one bit was incorrectly estimated to the total number of experiments. Note that we do not take degenerate errors [21] into consideration. They are treated as decoding failures.

In Figure 1, the decoding performance (f_m , FER) is plotted for each rate R (from left to right, $R = 0.75, 0.60, 0.50$) by varying the parameter P , where the number of physical qubits $n = ePL$ is proportional to P . Furthermore, high error-floor was not observed, at least down to an FER of 10^{-4} . No conventional quantum LDPC codes have been reported where the FER shows sharp threshold and no error floor down to 10^{-4} [22].

As P increases, we observe an exponential decrease in the FER. Additionally, a threshold phenomenon is evident, where the FER sharply drops as P grows, particularly when $f_m < f_m^*$ for some critical value f_m^* . We plotted circles at the thresholds f_m^* , which correspond to the points where the curves intersect, for each R .

In Figure 2, the pairs of thresholds and coding rates (f_m^*, R) are plotted. There is no conventional quantum error correction that achieves both a deep error floor and a threshold phenomenon [22]. Since conventional quantum error correction does not allow for a well-defined threshold, it is not included in this figure as a comparison. The results show that the proposed codes exhibit decoding performance that approaches the hashing bound.

4 Conclusions

We generalize the quantum error correcting code construction method [17] to general protograph matrices. By performing SP decoding that accounts for the correlation between X and Z errors, we achieved quantum error correction with both deep error floor and sharp threshold. Numerical experiments confirmed that the proposed method achieves error correction approaching the hashing bound, which serves as a benchmark for quantum error correction and represents the lower bound of the quantum capacity.

A Details of code construction

A.1 Generation of (\hat{H}_X, \hat{H}_Z)

In this section, we describe the construction method for orthogonal parity-check matrix pairs (\hat{H}_X, \hat{H}_Z) , where each matrix has column weight J , row weight L , and permutation matrices of size P as submatrices. It is known that non-binary LDPC codes with a column weight $J = 2$ exhibit good decoding performance. Therefore, in this

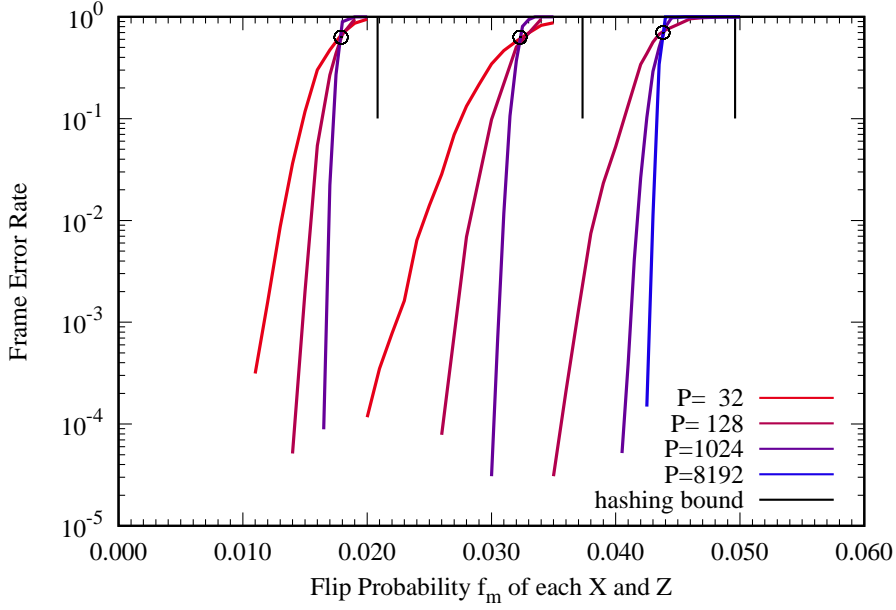


Figure 1: **Decoding performance of the proposed code: f_m vs. FER.** Decoding performance (f_m , FER) of the proposed code with $e = 8$, $J = 2$, $L \in \{8, 10, 16\}$, $P \in \{32, 128, 1024, 8192\}$, and $R \in \{0.50, 0.60, 0.75\}$. The black solid line indicates the hashing bound. The code length, that is, the number of physical bits, is given by $n = ePL$. It is evident that the proposed method simultaneously achieves both deep error floors and sharp thresholds.

paper, the column weight J is consistently set to $J = 2$. For a permutation mapping $f : \mathbb{Z}_P \rightarrow \mathbb{Z}_P = \{0, \dots, P - 1\}$, we denote by the uppercase $F \in \mathbb{F}_2^{P \times P}$, which is the permutation matrix of size P that has a 1 in the $(f(c), c)$ entry.

First, two sequences of permutations on \mathbb{Z}_P , $\underline{f} = (f_0, \dots, f_{L/2-1})$ and $\underline{g} = (g_0, \dots, g_{L/2-1})$, are chosen to satisfy the following three conditions (a), (b), and (c). Next, using \underline{f} and \underline{g} , the matrix pair (\hat{H}_X, \hat{H}_Z) is constructed as follows.

$$\hat{H}_X = \left[\begin{array}{cccc|cccc} F_0 & F_1 & \cdots & F_{L/2-1} & G_0 & G_1 & \cdots & G_{L/2-1} \\ F_{L/2-1} & F_0 & \cdots & F_{L/2-2} & G_{L/2-1} & G_0 & \cdots & G_{L/2-2} \end{array} \right]$$

$$\hat{H}_Z = \left[\begin{array}{cccc|cccc} G_0^\top & G_{L/2-1}^\top & \cdots & G_1^\top & F_0^\top & F_1^\top & \cdots & F_{L/2-1}^\top \\ G_1^\top & G_0^\top & \cdots & G_2^\top & F_1^\top & F_0^\top & \cdots & F_2^\top \end{array} \right]$$

This construction represents a natural generalization of the method proposed in [16].

- (a) (Commutativity): The elements of the arrays \underline{f} and \underline{g} are chosen so that they

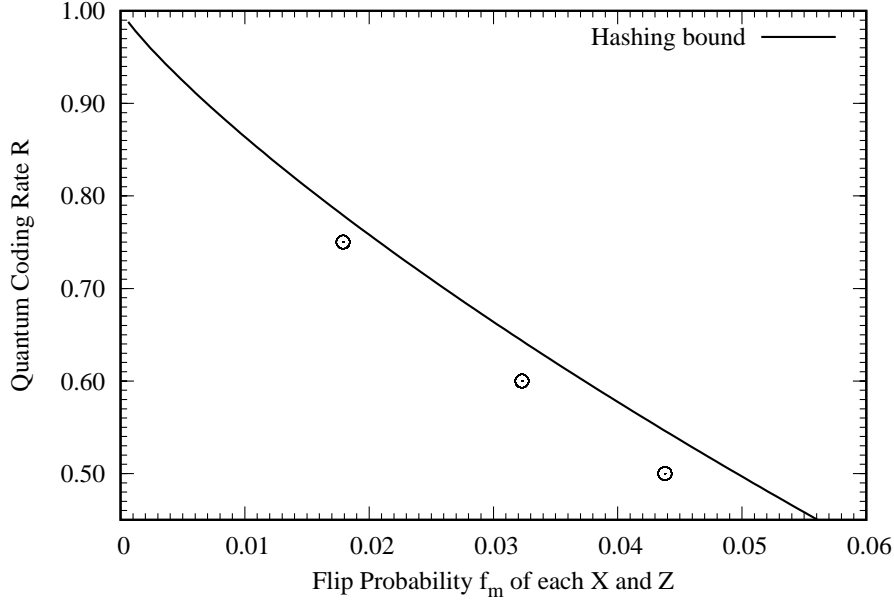


Figure 2: **Decoding performance of the proposed code: f_m vs. R .** The plot shows (f_m^*, R) , where f_m^* represents the threshold and R denotes the quantum coding rate. It can be observed that all rates approach the hashing bound.

commute with each other. Specifically, they satisfy ²

$$f_i \circ g_j(x) = g_j \circ f_i(x) \quad \text{for } 0 \leq i, j < L/2.$$

This condition ensures³ the orthogonality of \hat{H}_X and \hat{H}_Z . Since a cycle is formed along a specific path⁴ traversing all sub-matrices, it can be shown that the girth of this construction is upper-bounded by $2L$. The above conditions serve as sufficient conditions for the girth to achieve this upper bound.

- (b) (Achieving the girth upper bound $2L$): For $0 \leq l, l' < L/2$, $k \in \{0, \pm 1\}$, and $x \in \{0, \dots, P-1\}$,

$$f_l \circ g_{-l+k}(x) \neq f_{l'} \circ g_{-l'+k}(x),$$

where the subscripts of f and g are elements of $\mathbb{Z}_{L/2} = \{0, 1, \dots, L/2-1\}$. This condition is necessary to ensure that the process of generalization to non-binary codes, explained in the next section, does not fail. Under the condition

²This condition can actually be slightly relaxed as follows: f_{l-j} and f_{k-l} for $0 \leq l < L/2$ and $0 \leq j, k < J$ are commutative.

³For $0 \leq j, k < J$, $(\hat{H}_X \hat{H}_Z^T)_{j,k} = \sum_{l=0}^{L/2-1} (F_{-j+l} G_{k-l} + G_{k-l} F_{-j+l}) = O$.

⁴Two paths consist of a sequence of column sub-matrix indices of length $2L$, denoted as c_l^1 and c_l^2 for $l = 0, \dots, L-1$. For row sub-matrices, the traversal alternates vertically. Specifically, c_l^1 is defined as l when l is even and $L-l$ when l is odd, while c_l^2 is defined as l when l is even and $L-l+1$ when l is odd.

- (a), this condition becomes a necessary and sufficient condition for the girth to achieve the upper bound $2L$.
- (c) (Absence of short cycles): It is well known that the presence of short cycles in the Tanner graph defined by the matrices degrades the performance of the SP algorithm [23]. Conditions for the existence of short cycles in protograph matrices are well established [11]. The sets \underline{f} and \underline{g} are constructed to ensure that these conditions are not satisfied.

By incrementally adding elements of \underline{f} and \underline{g} one by one while satisfying the above three conditions, \underline{f} and \underline{g} can be efficiently constructed. In practice, it is preferable to construct \underline{f} and \underline{g} such that the submatrices are not general PMs but instead CPMs or APMs. Here, we describe the construction using matrices composed of general PMs to clarify the scope of the matrix classes where the above construction method is generally applicable.

For $J = 2$, $L = 4$, and $P = 9$, we provide examples of the above construction method. The arrays $\underline{f} = (x + 8, 7x + 7)$ and $\underline{g} = (x + 3, x + 6)$, constructed using CPMs, satisfy the conditions described above. Similarly, the sets $\underline{f} = (x + 1, x + 7)$ and $\underline{g} = (x + 1, x + 5)$, constructed using CPMs, also satisfy the conditions. In both cases, the girth of the resulting matrices \hat{H}_X and \hat{H}_Z is 8.

For $J = 2$, $L = 8$, $P = 6300$, $\underline{f} = (1051x + 2795, 4201x + 225, 1051x + 110, 2101x + 1675)$ and $\underline{g} = (5041x + 1122, 5041x + 4350, 3781x + 1686, 2521x + 2298)$ constructed using APMs, satisfy the conditions described above. The girth of the resulting matrices \hat{H}_X and \hat{H}_Z is 16, which provides an example exceeding the upper bound [10] of 12 for the girth of QC-LDPC codes.

A.2 Finite field extension to (H_Γ, H_Δ)

Let $q = 2^e$, and denote the finite field of size q by \mathbb{F}_q . In this section, we extend orthogonal binary protograph matrix pairs $(\hat{H}_X, \hat{H}_Z) \in \mathbb{F}_2^{P \times PL}$ constructed in the previous section to protograph matrix pairs $(H_\Gamma, H_\Delta) \in \mathbb{F}_q^{P \times PL}$. The finite field extension in this section are based on [17]. In [17], (\hat{H}_X, \hat{H}_Z) were assumed to be QC-LDPC matrices.

Kasai et al. [17] constructed orthogonal \mathbb{F}_q -valued protograph matrix pairs by replacing the entries of 1 in the QC-LDPC matrix pairs constructed by Hagiwara and Imai [16] with non-zero elements of \mathbb{F}_q . We generalize this method to transform protograph matrix pairs (\hat{H}_X, \hat{H}_Z) into orthogonal matrix pairs (H_Γ, H_Δ) over \mathbb{F}_q .

First, let us determine the non-zero entries (γ_{ij}) of H_Γ . Consider a one-dimensional array of length $2LP$, denoted as $\underline{\gamma} = (\gamma_0, \gamma_1, \dots, \gamma_{2LP-1})$, which satisfies the following conditions: for $0 \leq i < P$, $\gamma_{ij} = \gamma_j$, and for $P \leq i < 2P$, $\gamma_{ij} = \gamma_{j+PL/2}$. Assume that \mathbb{F}_q contains a primitive element α . Thus, \mathbb{F}_q can be written as $\mathbb{F}_q = \{0, \alpha^0, \alpha^1, \dots, \alpha^{q-2}\}$. We assume that the condition (a) is satisfied. Let us consider the condition for the existence of a non-zero H_Γ that satisfies the orthogonality equation $H_\Gamma H_\Delta^T = 0$, treating H_Γ as a variable. Denote $\underline{\lambda} \stackrel{\text{def}}{=} (\log_\alpha \gamma_0, \dots, \log_\alpha \gamma_{2LP-1})^T \in \mathbb{Z}_{q-1}^{2PL}$. When condition (b) holds, all-non-zero solution (γ_{ij}) of the equation $H_\Gamma H_\Delta^T =$

0 exist if and only if the following system of linear congruences over \mathbb{Z}_{q-1} with respect to $\underline{\lambda}$:

$$[-\hat{H}_Z^L \mid \hat{H}_Z^R \mid \hat{H}_Z^L \mid -\hat{H}_Z^R] \underline{\lambda} = \underline{0}, \quad (1)$$

where $\hat{H}_Z = [\hat{H}_Z^L \mid \hat{H}_Z^R]$ and each entry of the matrices takes a value in $\{0, \pm 1\} \subset \mathbb{Z}_{q-1}$.

The matrix in equation (1) can be transformed into its reduced row echelon form using elementary row operations without requiring division. By randomly selecting a random solution of this system, we obtain $\underline{\lambda}$ followed by $\underline{\gamma}$ and H_Γ . Furthermore, treating the non-zero entries of H_Δ as variables, the linear equation $H_\Gamma H_\Delta^\top = 0$ is solved to determine the non-zero entries of H_Δ .

An example of constructing (H_Γ, H_Δ) from (\hat{H}_X, \hat{H}_Z) is described in [17].

A.3 Conversion to (H_X, H_Z)

In this section, we construct orthogonal \mathbb{F}_2 -valued matrices $H_X, H_Z \in \mathbb{F}_2^{ePJ \times ePL}$ from the orthogonal \mathbb{F}_q -valued matrices $H_\Gamma, H_\Delta \in \mathbb{F}_q^{PJ \times PL}$ obtained in the previous section. The CSS code defined by these matrices H_X and H_Z is the quantum error-correcting code proposed in this paper.

Let $a(x) = a_0 + a_1x + \dots + a_e x^e$, where $a_0 = a_e = 1$ be the primitive polynomial for the primitive element $\alpha \in \mathbb{F}_q$. The companion matrix $A(\alpha)$ [24] for α is defined as follows:

$$A(\alpha) \stackrel{\text{def}}{=} \begin{bmatrix} 0 & 0 & 0 & 0 & a_0 \\ 1 & 0 & 0 & 0 & a_1 \\ 0 & 1 & 0 & 0 & a_2 \\ \vdots & \vdots & \ddots & \vdots & \vdots \\ 0 & 0 & 0 & 1 & a_{e-1} \end{bmatrix}.$$

We define the mapping $A : \mathbb{F}_q \rightarrow \mathbb{F}_2^{e \times e}$ as follows:

$$\begin{aligned} A(0) &\stackrel{\text{def}}{=} O, \\ A(\alpha^l) &\stackrel{\text{def}}{=} A(\alpha)^l \quad \text{for } l = 0, \dots, q-2. \end{aligned}$$

Using the mapping A , we construct (H_X, H_Z) as follows:

$$H_X = (A(\gamma_{i,j})), \quad H_Z = (A(\delta_{i,j})^\top).$$

From the properties of the companion matrix (Appendix B), it can be verified that (H_X, H_Z) are orthogonal.

$$\begin{aligned}
(H_X H_Z^\top)_{i,j} &= \sum_k A(\gamma_{i,k}) A(\delta_{k,j}) \\
&= \sum_k A(\gamma_{i,k} \delta_{k,j}) \\
&= A\left(\sum_k \gamma_{i,k} \delta_{k,j}\right) \\
&= A\left((H_\Gamma H_\Delta^\top)_{i,j}\right) \\
&= A(0) \\
&= O.
\end{aligned}$$

An example of constructing (H_X, H_Z) from (H_Γ, H_Δ) is described in [17].

B Properties of the companion matrix

Let $q = 2^e$. As known from [24], the mapping A is injective, and the image $A(\mathbb{F}_q)$ forms a field isomorphic to \mathbb{F}_q under the correspondence defined by A . The mapping satisfies the following properties:

$$\begin{aligned}
A(\gamma_1 + \gamma_2) &= A(\gamma_1) + A(\gamma_2), \\
A(\gamma_1 \gamma_2) &= A(\gamma_1) A(\gamma_2).
\end{aligned}$$

For $\gamma = \sum_{j=0}^{e-1} g_j \alpha^j \in \mathbb{F}_q$, the binary vector representation of γ is denoted as $\underline{v}(\gamma) := (g_0, \dots, g_{e-1})^\top \in \mathbb{F}_2^e$. This correspondence establishes a group isomorphism between \mathbb{F}_q and \mathbb{F}_2^e : $\underline{v}(\gamma_1 + \gamma_2) = \underline{v}(\gamma_1) + \underline{v}(\gamma_2)$.

The companion matrix $A(\alpha)$ can be expressed as:

$$A(\alpha) = (\underline{v}(\alpha^1), \underline{v}(\alpha^2), \dots, \underline{v}(\alpha^e)).$$

The first column of $A(\alpha^i)$ corresponds to $\underline{v}(\alpha^i)$.

The following properties hold:

$$\begin{aligned}
A(\gamma_1) \underline{v}(\gamma_2) &= \underline{v}(\gamma_1 \gamma_2), \\
A(\alpha^i) \underline{v}(\alpha^j) &= \underline{v}(\alpha^{i+j}) = \underline{v}(\alpha^i \alpha^j).
\end{aligned}$$

From this, the following equivalence holds:

$$\sum_j \gamma_j \delta_j = 0 \text{ iff } \sum_j A(\gamma_j) \underline{v}(\delta_j) = \underline{0}.$$

Define the mapping $A^\top : \mathbb{F}_q \rightarrow \mathbb{F}_2^{e \times e}$ as follows:

$$\begin{aligned}
A^\top(0) &\stackrel{\text{def}}{=} O, \\
A^\top(\alpha^i) &\stackrel{\text{def}}{=} (A(\alpha)^\top)^i \text{ for } i = 0, \dots, q-2.
\end{aligned}$$

The mapping A^\top is injective, and the image $A^\top(\mathbb{F}_q) \subset \mathbb{F}_2^{e \times e}$ forms a field that is isomorphic to \mathbb{F}_q under the correspondence defined by A^\top .

$$\begin{aligned} A^\top(\gamma_1 + \gamma_2) &= A^\top(\gamma_1) + A^\top(\gamma_2), \\ A^\top(\gamma_1\gamma_2) &= A^\top(\gamma_1)A^\top(\gamma_2). \end{aligned}$$

Define $\underline{w}(0) \stackrel{\text{def}}{=} (0, \dots, 0) \in \mathbb{F}_2^e$. Let $\underline{w}(\alpha^i) \in \mathbb{F}_2^e$ be defined as the first column of $A^\top(\alpha^i)$. This correspondence establishes a group isomorphism between \mathbb{F}_q and \mathbb{F}_2^e : $\underline{w}(\gamma_1 + \gamma_2) = \underline{w}(\gamma_1) + \underline{w}(\gamma_2)$. The following properties hold:

$$\begin{aligned} A^\top(\gamma_1)\underline{w}(\gamma_2) &= \underline{w}(\gamma_1\gamma_2), \\ A^\top(\alpha^i)\underline{w}(\alpha^j) &= \underline{w}(\alpha^{i+j}) = \underline{w}(\alpha^i\alpha^j). \end{aligned}$$

From this, the following equivalence holds:

$$\sum_j \gamma_j \delta_j = 0 \text{ iff } \sum_j A^\top(\gamma_j)\underline{w}(\delta_j) = \underline{0}.$$

i	0	1	2	3	4	5	6
α^i	α^0	α^1	α^2	α^3	α^4	α^5	α^6
$\underline{w}(\alpha^i)$	$(100)^\top$	$(010)^\top$	$(001)^\top$	$(110)^\top$	$(011)^\top$	$(111)^\top$	$(101)^\top$
A^i	$\begin{pmatrix} 100 \\ 010 \\ 001 \end{pmatrix}$	$\begin{pmatrix} 001 \\ 101 \\ 010 \end{pmatrix}$	$\begin{pmatrix} 010 \\ 011 \\ 101 \end{pmatrix}$	$\begin{pmatrix} 101 \\ 111 \\ 011 \end{pmatrix}$	$\begin{pmatrix} 011 \\ 110 \\ 111 \end{pmatrix}$	$\begin{pmatrix} 111 \\ 100 \\ 110 \end{pmatrix}$	$\begin{pmatrix} 110 \\ 001 \\ 100 \end{pmatrix}$
$\underline{w}(\alpha^i)$	$(100)^\top$	$(001)^\top$	$(010)^\top$	$(101)^\top$	$(011)^\top$	$(111)^\top$	$(110)^\top$
$(A^\top)^i$	$\begin{pmatrix} 100 \\ 010 \\ 001 \end{pmatrix}$	$\begin{pmatrix} 010 \\ 001 \\ 110 \end{pmatrix}$	$\begin{pmatrix} 001 \\ 110 \\ 011 \end{pmatrix}$	$\begin{pmatrix} 110 \\ 011 \\ 111 \end{pmatrix}$	$\begin{pmatrix} 011 \\ 111 \\ 101 \end{pmatrix}$	$\begin{pmatrix} 111 \\ 101 \\ 100 \end{pmatrix}$	$\begin{pmatrix} 101 \\ 100 \\ 010 \end{pmatrix}$

Figure 3: Companion matrices and binary representation for primitive element $\alpha \in \mathbb{F}_8$ with primitive polynomial $a(x) = 1 + x + x^3$.

C Details of decoding methods

C.1 Decoding algorithm

Let $M = PJ$, $N = PL$, and $n = eN$. Using the matrices $H_X, H_Z \in \mathbb{F}_2^{M \times eN}$ and $H_\Gamma, H_\Delta \in \mathbb{F}_q^{M \times N}$ provided in the previous sections, we describe the method for performing error correction. The decoding process involves estimating the noise vectors $\underline{x}, \underline{z} \in \mathbb{F}_2^{eN}$ from the syndromes $\underline{s} = H_X \underline{x}$ and $\underline{t} = H_Z \underline{z}$, where the matrices H_X and H_Z are constructed from the non-binary matrices H_Γ and H_Δ as described in the previous section.

By leveraging the structure of H_Γ and H_Δ over \mathbb{F}_q , the proposed method aims to improve decoding performance by interpreting the binary matrices H_X and H_Z as derived from non-binary protograph-based LDPC codes. For $n = eN$ qubits, the vector representations of X and Z errors are denoted by \underline{x} and \underline{z} , respectively. The role of the decoder is to estimate the noise vectors $\underline{x}, \underline{z} \in \mathbb{F}_2^{eN}$ from the syndromes $\underline{s} = H_X \underline{x}, \underline{t} = H_Z \underline{z} \in \mathbb{F}_2^{eM}$.

We divide \underline{x} and \underline{z} into e -bit segments and write:

$$\underline{x} = (x_1, \dots, x_N), \quad \underline{z} = (z_1, \dots, z_N).$$

We assume a depolarizing channel with error probability p_D . Hashing bound for the depolarizing channel with error probability p_D is given as follows:

$$R = 1 - H(p_D, p_D/3, p_D/3, p_D/3) = 1 + (1 - 3p_D) \log_2(1 - 3p_D) + 3p_D \log_2(p_D),$$

where $H(\cdot)$ is the entropy function. The probability of occurrence for $\underline{x}, \underline{z} \in \mathbb{F}_2^{eN}$ in this channel is given by the following expression:

$$\begin{aligned} p(\underline{x}, \underline{z}) &= \prod_{j=1}^N p(x_j, z_j), \\ p(x_j, z_j) &= \prod_{k=1}^e p(x_j^k, z_j^k), \\ p(x, z) &= \begin{cases} 1 - p_D, & (x, z) = (0, 0), \\ \frac{p_D}{3}, & (x, z) = (0, 1), (1, 0), (1, 1), \end{cases} \end{aligned}$$

where $x_j^k, z_j^k \in \mathbb{F}_2$ are the k -th bit of x_j, z_j , respectively.

The posterior probability of $\underline{x}, \underline{z}$ given the syndromes $\underline{s}, \underline{t}$ can be sparsely factorized as follows:

$$p(\underline{x}, \underline{z} | \underline{s}, \underline{t}) \propto \left(\prod_{i=1}^M \mathbb{1} \left[\sum_{j=1}^N (H_X)_{ij} x_j = s_i \right] \right) \left(\prod_{i=1}^M \mathbb{1} \left[\sum_{j=1}^N (H_Z)_{ij} z_j = t_i \right] \right) \left(\prod_{j=1}^N p(x_j, z_j) \right), \quad (2)$$

where $(H_X)_{ij}, (H_Z)_{ij}$ denotes the (i, j) -th $(e \times e)$ submatrix of H_X, H_Z , respectively. We denote $\mathbb{1}[\cdot]$ as 1 if the inside the brackets is true, and 0 otherwise. For each i , note that there are L values of j for which $(H_X)_{ij}$ and $(H_Z)_{ij}$ are non-zero, respectively.

Using this sparsely-factorized posterior probability, approximate marginalization is performed using the SP algorithm [20]. The proposed decoding method estimates the noise by selecting the noise vector for each e -bit segment that maximizes the marginalized posterior probability.

The SP algorithm that marginalizes this posterior probability (2), specifically, is an algorithm that updates the following eight types of messages:

$$\mu_{ij}^X(x_j), \mu_{ij}^Z(z_j), \nu_{ji}^X(x_j), \nu_{ji}^Z(z_j), \lambda_j^X(x_j), \lambda_j^Z(z_j), \kappa_j^X(x_j), \kappa_j^Z(z_j).$$

All messages are initialized to a uniform distribution over x_j and z_j . Each message is updated using the following update equations. After each update, the messages are normalized to ensure they form probability distributions.

$$\nu_{ij}^X(x_j) = \sum_{(x_{j'}): j' \in \partial_X(i) \setminus j} \mathbb{1} \left[\sum_{j' \in \partial_X(i)} (H_X)_{ij'} x_{j'} = s_i \right] \prod_{j' \in \partial_X(i) \setminus j} \mu_{j'i}^X(x_{j'}), \quad (3)$$

$$\nu_{ij}^Z(z_j) = \sum_{(z_{j'}): j' \in \partial_Z(i) \setminus j} \mathbb{1} \left[\sum_{j' \in \partial_Z(i)} (H_Z)_{ij'} z_{j'} = t_i \right] \prod_{j' \in \partial_Z(i) \setminus j} \mu_{j'i}^Z(z_{j'}), \quad (4)$$

$$\lambda_j^X(x_j) = \prod_{i \in \partial_X(j)} \nu_{ij}^X(x_j),$$

$$\lambda_j^Z(z_j) = \prod_{i \in \partial_Z(j)} \nu_{ij}^Z(z_j),$$

$$\kappa_j^X(x_j) = \sum_{z_j} p(x_j, z_j) \lambda_j^Z(z_j),$$

$$\kappa_j^Z(z_j) = \sum_{x_j} p(x_j, z_j) \lambda_j^X(x_j),$$

$$\mu_{ji}^X(x_j) = \kappa_j^X(x_j) \prod_{i' \in \partial_X(j) \setminus i} \nu_{i'j}^X(x_j), \quad (5)$$

$$\mu_{ji}^Z(z_j) = \kappa_j^Z(z_j) \prod_{i' \in \partial_Z(j) \setminus i} \nu_{i'j}^Z(z_j), \quad (6)$$

where $\partial_X(i)$ and $\partial_Z(i)$ are the set of column index j such that $(H_X)_{ij} \neq O$ and $(H_Z)_{ij} \neq O$, respectively. Similarly, $\partial_X(j)$ and $\partial_Z(j)$ are the set of row index i such that $(H_X)_{ij} \neq O$ and $(H_Z)_{ij} \neq O$, respectively. It holds that $\#\partial_X(i) = \#\partial_Z(i) = J$ and $\#\partial_X(j) = \#\partial_Z(j) = L$.

After the pre-determined number of updates, the estimated noise

$$\hat{x}_j = \operatorname{argmax}_{x_j} \prod_{i \in \partial_X(j)} \nu_{ij}^X(x_j), \quad \hat{z}_j = \operatorname{argmax}_{z_j} \prod_{i \in \partial_Z(j)} \nu_{ij}^Z(z_j)$$

are checked if they satisfy the syndromes s_i, t_i . Specifically, if they satisfy

$$\sum_{j \in \partial_X(i)} (H_X)_{ij} \hat{x}_j = s_i, \quad \sum_{j \in \partial_Z(i)} (H_Z)_{ij} \hat{z}_j = t_i,$$

then (\hat{x}_j) and (\hat{z}_j) are accepted as the estimated noise, and the algorithm terminates. If the syndrome are not satisfied, a decoding failure is declared.

The messages (3) and (4) can be computed using FFT [18], requiring $O(Lq \log q)$ operations per message. This message computation can also be implemented as a decoding method for LDPC codes over a finite field. The detail is provided in Appendix C.2. On the other hand the computation for messages (5) and (6) require q^2 operations per message. Other messages computation require only $O(Jq)$ operations per message.

Since performance improves by increasing P , and assuming q is fixed, the overall computational complexity is proportional to the number of physical qubits $n = ePL$.

C.2 Sum-product algorithm over finite field

We show $p(\underline{x}, \underline{z} | \underline{s}, \underline{t})$ can also be expressed using elements of a finite field as follows:

$$p(\underline{x}, \underline{z} | \underline{s}, \underline{t}) \propto \left(\prod_{i=1}^M \mathbb{1} \left[\sum_{j=1}^N \gamma_{ij} \xi_j = \sigma_i \right] \right) \left(\prod_{i=1}^M \mathbb{1} \left[\sum_{j=1}^N \delta_{ij} \zeta_j = \tau_i \right] \right) \left(\prod_{j=1}^N p(x_j, z_j) \right).$$

For $s_i, t_i, x_j, z_j \in \mathbb{F}_2^e$, we define $\sigma_i, \tau_i, \xi_j, \zeta_j \in \mathbb{F}_q$ are such that $\underline{v}(\sigma_i) = s_i, \underline{w}(\tau_i) = t_i, \underline{v}(\xi_j) = x_j$ and $\underline{w}(\zeta_j) = z_j$ hold. Note that $\underline{v}(\cdot)$ and $\underline{w}(\cdot)$ were defined in B.

From Bayes' rule and the fact that the observed syndromes $\underline{s}, \underline{t}$ can be treated as constants, we have:

$$\begin{aligned} p(\underline{x}, \underline{z} | \underline{s}, \underline{t}) &= p(\underline{s}, \underline{t} | \underline{x}, \underline{z}) p(\underline{x}, \underline{z}) / p(\underline{s}, \underline{t}) \\ &\propto p(\underline{s}, \underline{t} | \underline{x}, \underline{z}) p(\underline{x}, \underline{z}). \end{aligned}$$

Next, using the chain rule and the fact that the syndromes are determined by the noise, we obtain:

$$\begin{aligned} p(\underline{s}, \underline{t} | \underline{x}, \underline{z}) &= p(\underline{s}, \underline{t} | \underline{x}, \underline{z}) \\ &= p(\underline{s} | \underline{t}, \underline{x}, \underline{z}) p(\underline{t} | \underline{x}, \underline{z}) \\ &= p(\underline{s} | \underline{x}) p(\underline{t} | \underline{z}). \end{aligned}$$

From the fact that the noise and syndromes are determined by the parity-check equations and the properties of the parity-check matrices, we have:

$$\begin{aligned} p(\underline{s} | \underline{x}) &= \prod_{i=1}^M \mathbb{1} \left[\sum_{j=1}^N (H_X)_{ij} x_j = s_i \right] \\ &= \prod_{i=1}^M \mathbb{1} \left[\sum_{j=1}^N A(\gamma_{ij}) x_j = s_i \right] \\ &= \prod_{i=1}^M \mathbb{1} \left[\sum_{j=1}^N A(\gamma_{ij}) \underline{v}(\xi_j) = \underline{v}(\sigma_i) \right] \\ &= \prod_{i=1}^M \mathbb{1} \left[\sum_{j=1}^N \gamma_{ij} \xi_j = \sigma_i \right]. \end{aligned}$$

For similar reasons, we obtain the following. Note that the companion matrix is given

by A^\top and the vector representation is given by $\underline{w}(\cdot)$:

$$\begin{aligned}
p(\underline{t}|\underline{z}) &= \prod_{i=1}^M \mathbb{1}\left[\sum_{j=1}^N (H_Z)_{ij} z_j = t_i\right] \\
&= \prod_{i=1}^M \mathbb{1}\left[\sum_{j=1}^N A^\top(\delta_{ij}) z_j = t_i\right] \\
&= \prod_{i=1}^M \mathbb{1}\left[\sum_{j=1}^N A^\top(\delta_{ij}) \underline{w}(\zeta_j) = \underline{w}(\tau_i)\right] \\
&= \prod_{i=1}^M \mathbb{1}\left[\sum_{j=1}^N \delta_{ij} \zeta_j = \tau_i\right].
\end{aligned}$$

References

- [1] D. Bluvstein, S. J. Evered, A. A. Geim, S. H. Li, H. Zhou, T. Manovitz, S. Ebadi, M. Cain, M. Kalinowski, D. Hangleiter *et al.*, “Logical quantum processor based on reconfigurable atom arrays,” *Nature*, vol. 626, no. 7997, pp. 58–65, 2024.
- [2] R. Feynman, “Simulating physics with computers,” *International Journal of Theoretical Physics*, vol. 21, no. 6-7, pp. 467–488, Jun. 1982. [Online]. Available: <http://dx.doi.org/10.1007/bf02650179>
- [3] J. Preskill, “Quantum computing in the NISQ era and beyond,” *Quantum*, vol. 2, p. 79, 2018.
- [4] R. Gallager, “Low-density parity-check codes,” *IRE Transactions on information theory*, vol. 8, no. 1, pp. 21–28, 1962.
- [5] S. Kudekar, T. Richardson, and R. Urbanke, “Spatially coupled ensembles universally achieve capacity under belief propagation,” in *2012 IEEE International Symposium on Information Theory Proceedings*, 2012, pp. 453–457.
- [6] S. Lloyd, “Capacity of the noisy quantum channel,” *Physical Review A*, vol. 55, no. 3, p. 1613, 1997.
- [7] P. Shor, “The quantum channel capacity and coherent information,” in *Lecture Notes, MSRI Workshop on Quantum Computation*, 2002.
- [8] I. Devetak, “The private classical capacity and quantum capacity of a quantum channel,” *IEEE Transactions on Information Theory*, vol. 51, no. 1, pp. 44–55, 2005.
- [9] J. Thorpe, “Low-density parity-check (ldpc) codes constructed from protographs,” *IPN progress report*, vol. 42, no. 154, pp. 42–154, Aug. 2003.

- [10] M. P. Fossorier, “Quasicyclic low-density parity-check codes from circulant permutation matrices,” *IEEE transactions on information theory*, vol. 50, no. 8, pp. 1788–1793, 2004.
- [11] S. Myung, K. Yang, and D. S. Park, “A combining method of structured LDPC codes from affine permutation matrices,” in *2006 IEEE International Symposium on Information Theory*. IEEE, 2006, pp. 674–678.
- [12] R. Yoshida and K. Kasai, “Linear permutation polynomial codes,” in *2019 IEEE International Symposium on Information Theory (ISIT)*, 2019, pp. 66–70.
- [13] M. C. Davey and D. J. MacKay, “Low density parity check codes over $gf(q)$,” in *1998 Information Theory Workshop (Cat. No. 98EX131)*. IEEE, 1998, pp. 70–71.
- [14] A. R. Calderbank and P. W. Shor, “Good quantum error-correcting codes exist,” *Physical Review A*, vol. 54, no. 2, p. 1098, 1996.
- [15] A. M. Steane, “Error correcting codes in quantum theory,” *Physical Review Letters*, vol. 77, no. 5, p. 793, 1996.
- [16] M. Hagiwara and H. Imai, “Quantum quasi-cyclic LDPC codes,” in *2007 IEEE International Symposium on Information Theory*. IEEE, 2007, pp. 806–810.
- [17] K. Kasai, M. Hagiwara, H. Imai, and K. Sakaniwa, “Quantum error correction beyond the bounded distance decoding limit,” *IEEE Transactions on Information Theory*, vol. 58, no. 2, pp. 1223–1230, 2011.
- [18] D. J. MacKay, G. Mitchison, and P. L. McFadden, “Sparse-graph codes for quantum error correction,” *IEEE Transactions on Information Theory*, vol. 50, no. 10, pp. 2315–2330, 2004.
- [19] P. W. Shor, “Scheme for reducing decoherence in quantum computer memory,” *Physical review A*, vol. 52, no. 4, p. R2493, 1995.
- [20] F. R. Kschischang, B. J. Frey, and H.-A. Loeliger, “Factor graphs and the sum-product algorithm,” *IEEE Transactions on information theory*, vol. 47, no. 2, pp. 498–519, 2001.
- [21] H. Yao, W. A. Laban, C. Häger, A. G. i. Amat, and H. D. Pfister, “Belief propagation decoding of quantum LDPC codes with guided decimation,” in *2024 IEEE International Symposium on Information Theory (ISIT)*, 2024, pp. 2478–2483.
- [22] L. Hanzo, Z. Babar, Z. Cai, D. Chandra, I. B. Djordjevic, B. Koczor, S. X. Ng, M. Razavi, and O. Simeone, “Quantum information processing, sensing and communications: Their myths, realities and futures,” *arXiv preprint arXiv:2412.00987*, 2024.
- [23] R. Asvadi, A. H. Banihashemi, and M. Ahmadian-Attari, “Lowering the error floor of ldpc codes using cyclic liftings,” *IEEE Transactions on information theory*, vol. 57, no. 4, pp. 2213–2224, 2011.

- [24] F. J. MacWilliams and N. J. A. Sloane, "The theory of error-correcting codes," 1977.